

Opto-electronic system for displacement and vibration measurements

Cite as: Review of Scientific Instruments 58, 1678 (1987); <https://doi.org/10.1063/1.1139367>
Submitted: 09 February 1987 . Accepted: 20 March 1987 . Published Online: 04 June 1998

F. Francini, M. Macchiarulo, B. Tiribilli, and P. K. Buah-Bassuah



View Online



Export Citation



New

Your Qubits. Measured.

Meet the next generation of quantum analyzers

- Readout for up to 64 qubits
- Operation at up to 8.5 GHz, mixer-calibration-free
- Signal optimization with minimal latency

[Find out more](#)



Opto-electronic system for displacement and vibration measurements

F. Francini, M. Macchiarulo, B. Tiribilli,^{a)} P. K. Buah-Bassuah^{b)}

Istituto Nazionale di Ottica, Largo E. Fermi 6, I-50125 Firenze, Italy

(Received 9 February 1987; accepted for publication 20 March 1987)

A device capable of measuring small displacements and vibrations of a moving body is presented. A small mirror, firmly attached to the object under investigation, deflects a pair of laser beams onto two distinct photodetectors. From the examination of the output signals, it is possible to have separate information on the rotational and translational movements of a surface.

INTRODUCTION

In this paper, we present an opto-electronic device which has been developed with the aim of measuring small displacements of a moving object. This device is very promising for applications concerning the accurate measurement of vibrations and the positioning of mechanical pieces. It can be compared directly with the accelerometer, but it has the advantage of a frequency response starting from dc and, furthermore, it is a noncontact device. This last characteristic of our device extends the measurement possibilities to those circumstances which require carrying out vibrational tests on rotating bodies, as in the case of motor shafts; this excludes the direct use of the accelerometer.

I. THE SENSOR

The principal component of this opto-electronic device is a particular type of semiconductor sensor called a position sensing photodetector (PSD). The function of this sensor is based on the principle of the lateral photoeffect.¹⁻⁴ Each time a light spot strikes the surface of the photodetector, the surface currents are collected by four electrodes displaced along the Cartesian axes.

The equivalent circuit of the PSD is shown in Fig. 1, where I_s is the photocurrent generated by the light incident on the semiconductor. R_{s1} and R_{s2} , on the other hand, represent the resistive sheets of the front and back surface of the detector where the electrodes of the x and y axes are connected in pairs. I_1 , I_2 , I_3 , and I_4 are the output currents of the four electrodes. Therefore, the position on the x axis is proportional to $(I_2 - I_1)$ and that on the y axis to $(I_4 - I_3)$. In order to obtain an output signal unaffected by the light intensity, these quantities are divided by the sum of the photocurrents along the corresponding axes so that

$$x \text{ position} = (I_2 - I_1) / (I_2 + I_1),$$

$$y \text{ position} = (I_4 - I_3) / (I_4 + I_3).$$

In the experiments reported, a UDT-SC10D photodetector was used.

II. THE DEVICE

The technique of using this device consists of fixing a small mirror on the object under investigation, at the point

where one wants to take the measurement.

A laser beam is incident on the mirror at a certain angle and then deflected onto the surface of the PSD. A translation of the surface of the object or a different orientation causes further deflection of the beam which, therefore, impinges at a different point on the photodetector.

The variation of the position of the beams is detected by the different photocurrents in the four electrodes of the detector. It is quite evident that the longitudinal translation is indistinguishable from the rotation of the body; it is, therefore, necessary to employ an appropriate optical configuration that would make the movement of the components distinctly separate.

Figure 2 shows the sketch of the device from which it is possible to have information for the translation and rotational movements of the object. The laser beam B_0 is split by the cube splitter CS into two beams namely, B_1 and B_2 . A mirror is fixed to the surface of the object under test S, and M_2 deflects B_2 onto S. The beam B_1 , that is incident normally on S, is not deflected by translational motion D , thus the sensor PSD1 will solely detect the rotational movement α of the surfaces. The beam B_2 incident on S at an angle φ , is then deflected onto PSD2 from the joint effect of the rotation of an angle α and the translational displacement D . If L is the distance between the surface S and the photodetector, a general movement d of the laser beam deflected from S can be derived with the final and general equation represented as follows:

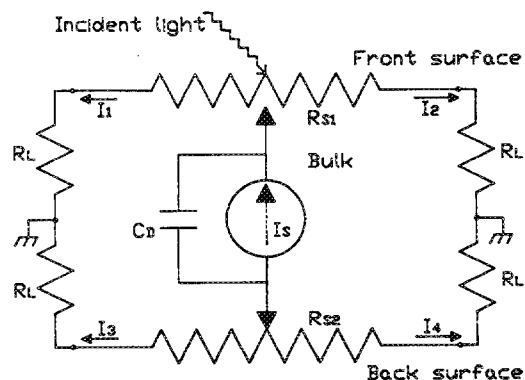


FIG. 1. Equivalent circuit of the photodetector. RL are load resistances.

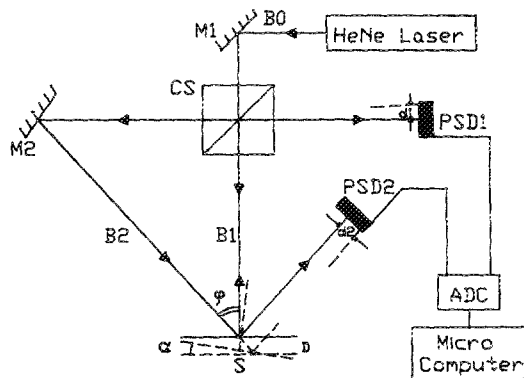


FIG. 2. Block diagram of the optical device.

$$d = 2D \sin \varphi + [D(\cos 2\varphi / \cos \varphi) + L] \tan 2\alpha, \quad (1)$$

where φ is the initial rotation of the surface S .

In the case when $L \gg D$, $\varphi = 0^\circ$, Eq. (1) becomes

$$d_1 = L \tan 2\alpha. \quad (2)$$

If instead $\varphi \neq 0^\circ$, and $L \gg D$, from Eq. (1) we have

$$d_2 = 2D \sin \varphi + L \tan 2\alpha. \quad (3)$$

Under the conditions described above, the output currents I_1 and I_2 from the two photodetectors are proportional to the quantities expressed in Eqs. (2) and (3). From I_1 , the value of α could be directly calculated and that of D could be evaluated from the difference between I_1 and I_2 .

In order for the system to be more compact, the mirror M_2 was substituted with a prism P and the lens L that deflects the beam B_2 at an angle α , depending on the numerical aperture. The lens L has a hole at its center so that the laser beam can be freely deflected through it onto the surface S (Fig. 3).

The device described above, consisting of optical and electronic parts relative to the sensors, was also equipped with the section dedicated to data acquisition and processing. An Olivetti computer (M24) was interfaced with a 12-bit, 4-input analog/digital converter and connected to the x and y output of the photodetectors.

With this system, it was possible to acquire data with a sampling time of $30 \mu\text{s}$ reliably enough to analyze signals of frequency higher than 3 kHz.

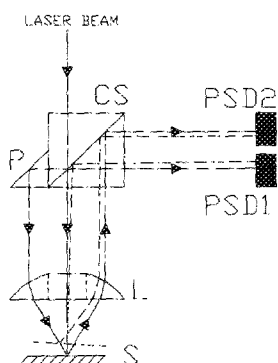


FIG. 3. The optical probe.

The limit of the system with respect to frequency is of the order of 10 kHz, and the principal limitation consists of the photodetector and the dedicated analog electronics.

There is no practical limit to the measured minimum frequency because all the systems are dc coupled. Obviously, in this case also, the limitation is due to the long-term drifts of the electronic components. In this device, with $L = 40 \text{ cm}$ and $\alpha = 30^\circ$, rotational and translational sensitivities of 0.005 deg/V and $100 \mu\text{m/V}$ were measured, respectively.

III. MEASUREMENT

The first cycle of measurements was taken with a small and very light mirror (diameter 5 mm and weight 0.01 g) which was stuck firmly on the moving membrane of a loud-speaker and served as a means of verifying the method.

More precisely, a combined translation and rotation were impressed on the mirror by superposing the independent movements of two loudspeakers. The small high-frequency speaker to which the mirror was attached had its membrane fixed rather closely to the support rim at its outer edge; this edge, therefore, remained essentially fixed while the center was free to move to and fro when the coil was excited. The effect was to rotate the mirror through an angle α , since it was attached to the membrane at a point between the edge and the center. The small speaker was mounted as a unit on a large low-frequency speaker; the membrane in this case was loosely attached at the outer rim so that there was no rotation, and the assembly was, in any case, mounted at the center. The total effect was that the mirror was translated at lower frequencies by the large speaker and rotated at high frequencies by the small speaker, and the rotation and translation could be independently controlled.

Figure 4 (a) represents the displacement of the beam B_2 on the photodetector PSD2 from the loudspeaker system which jointly gave the rotational and the translational effect. The small loudspeaker is driven by a sinusoidal signal of

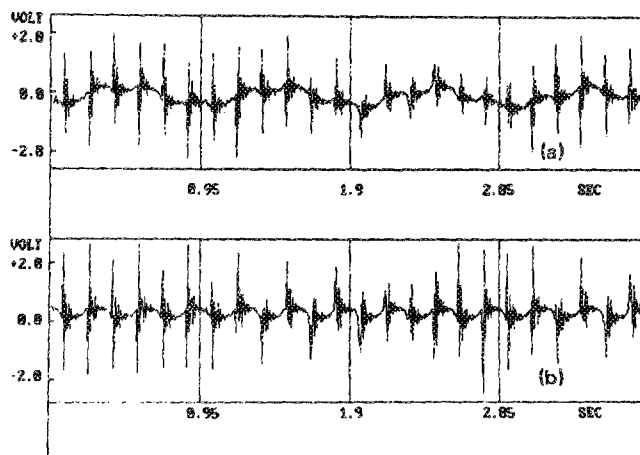


FIG. 4. (a) Signal arising from the displacement of the beam B_2 on the photodetector PSD2. The signal is given jointly by rotational and translational effect of the surface. (b) Signal arising from the displacement of the beam B_1 on the photodetector PSD1 by the signal is given only by the rotational effect.

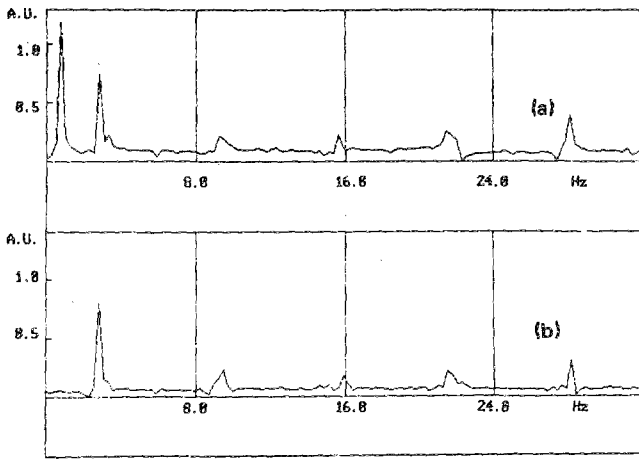


FIG. 5. (a) Frequency spectrum of the signal relative to Fig. 4 (a). (b) Frequency spectrum of the signal relative to Fig. 4 (b).

frequency 3 Hz. At this frequency, the response of the small loudspeaker is not linear since the movement of the membrane is more irregular as it is observed from the signal [Fig. 4 (a)]. The large loudspeaker was instead driven by a sinusoidal signal of frequency 1 Hz. Figure 4 (b) represents the displacement of beam *B*₁ on the photodetector PSD1. In this case, it is evident that there was only a rotational effect. Figure 5 shows the relative frequency spectrum of the two channels of our device. This spectrum was calculated considering the total displacements on the photodetector, that is, the resultant of the data acquisition on *x* and *y* axes.

Figure 5 (a) shows the output spectrum of oscillation α of PSD1, while Fig. 5 (b) shows also the output spectrum of PSD2. The comparison between the two spectra shows the translational effect of the large loudspeaker because an extra line at low frequencies can be observed.

The second cycle of measurements refers to the rotational vibrations of the shaft of an electric motor, mounted

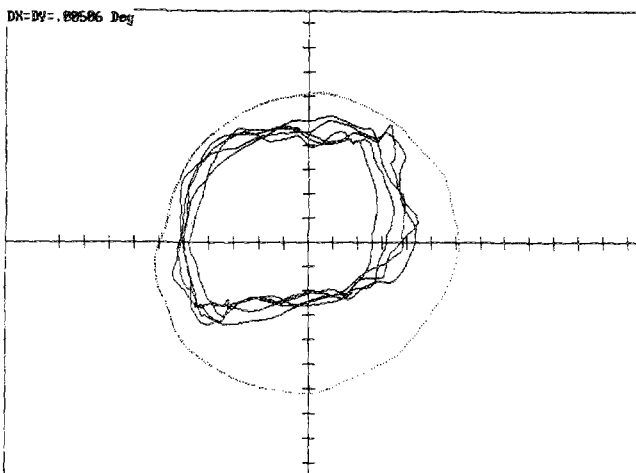


FIG. 6. Behavior of the angular oscillation of the shaft of an electric motor. The external curve is relative to the velocity of 50 rev/s. The internal curve is relative to the velocity of 150 rev/s.

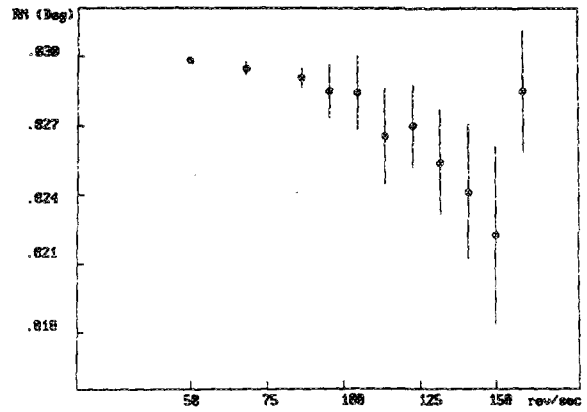


FIG. 7. Behavior of the mean radius for different rotational velocity.

on an elastic structure. The experimental setup is similar to the previous one except that the small mirror remained stuck at the end of the shaft of the electric motor. In this setup, if the end of the shaft is not rotating perpendicular to the axis of rotation, or the mirror was not attached exactly on its plane, the reflected laser beam during the rotation of the shaft describes a cone, that is, a circle on the surface of the photodetector.

In order to avoid problems arising from this fact in the interpretation of the results, we must consider the circle described on the detector as the reference line or zero line and evaluate the deviation from this reference line as the actual noisy trajectory in the experiment. In our case, as the vibration of the axis appeared at high velocity the circle described at the low speed was considered as the reference line.

Figure 6 shows the behavior of the oscillations of the shaft of the motor for two different rotational velocities. The external curve is relative to the velocity of 50 rev/s, sufficiently small not to have vibrations. The internal curve, relative to the velocity of 150 rev/s, is seen to correspond to a perturbed beam path on account of the vibrations.

Figure 7 represents the behavior of the mean radius for different rotational velocities of the motor. The vertical line

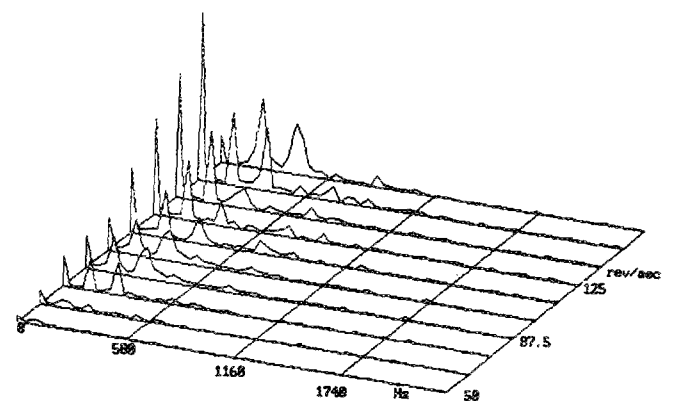


FIG. 8. Frequency spectra of the signals relative to Fig. 7. Intensity of spectra are in arbitrary units.

through the circle represents the noise of the mean radius, which is represented as the rms amplitude of oscillation.

Figure 6 shows that we have a sinusoidal waveform in the presence of noise. The sinusoidal period is bound to the rotational velocity and decreases with increasing velocity. In order to extract the contribution due only to vibrations, it is necessary to scale the reference time of oscillation because it is comparable with the period of the curve under investigation. The data shown in Fig. 7 have been analyzed in the frequency domain in order to show the presence of harmonics and their frequency spectra for different rotational velocities are given in Fig. 8.

ACKNOWLEDGMENT

The authors acknowledge Professor F. T. Arecchi for useful discussions.

^{a)} Present address: Officine Galileo, Campi Bisenzio, Firenze, Italy.

^{b)} Permanent address: Department of Physics, University of Cape Coast, Cape Coast, Ghana.

¹⁾ J. T. Wallmark, Proc. IRE 45, 474 (1957).

²⁾ R. B. Emmons, Solid State Electron. 10, 505 (1967).

³⁾ H. J. Woltring, IEEE Trans. Electron. Devices ED-22, 581 (1975).

⁴⁾ G. Petersson and L. F. Linholm, IEEE J. Solid State Circuits SC-13, 392 (1978).